Surface interactions between nanocrystal cellulose and liposomes

by

Min Li

A thesis
presented to the University of Waterloo
in the fulfillment of the
thesis requirement for the degree of
Master of Applied Science
in
Chemical Engineering (Nanotechnology)

Waterloo, Ontario, Canada, 2015

Author's Declaration

I hereby declare that I am the sole author of this thesis. This is a true copy of the

thesis, including any required final revisions, as accepted by my examiners.

I understand that my thesis may be made electronically available to the public

Abstract

Cellulose nanocrystal (CNC)，which is produced from acid hydrolysis of native cellulose fibers, is a nanoparticle with exceptional strength and physicochemical characteristics. It is renewable, biodegradable, non-toxic and environmentally friendly. Due to its advantages, many chemical modifications on the surface of CNC were performed for different applications, for example, enzyme immobilization, catalyst, antimicrobial medical applications and drug delivery.

In order to design a good drug delivery system, the most important thing is to figure out the surface interaction between different systems. This thesis is focused on the modification of CNC and the surface interactions between two types of CNC (cationic and anionic CNC) and three varieties of liposomes. The cationic CNC used in this study is glycidylltrimethylammonium chloride (GTMAC) grafted CNC, while the anionic CNCs are pristine CNC and TEMPO CNC respectively.

Liposomes are composed of phospholipids bilayers in concentric layers, similar to the microspheres of cell membrane. It has many advantages as a drug carrier, such as extending the efficacy, reducing drug toxicity, improving curative effect and avoiding tolerance. The three types of liposomes used are DOPC=, DOTAP and DOPG. The liposomes were mixed with CNCs and their interactions were examined and elucidated.

In this thesis, the adsorption between CNC and liposomes has been proven

in certain conditions. CNC has no damage to the membrane of the liposomes. In addition, the interactions between this system have been confirmed as electrostatic interactions due to effect of salt. However, one big problem is that the size of the complex is quite hard to control.

Acknowledgement

Firstly, I would like to express my thanks to my supervisors, Dr. Tam and Dr. Liu, for their helpful advice, patient guidance and constant encouragement during my research and in writing the thesis. Their patience and enthusiasm encouraged me when I encountered difficulties in my research. I deeply appreciate the chance to study and work under their supervision.

Secondly, I would like to thank all the members in my lab, Dr. Shi, Yibo Liu, Li Chen, Debbie Wu, Feng Wang, Biwu Liu, Po-Jung Jimmy Huang. With their discussions, suggestions and help, I am able to successfully complete my thesis research.

Last but not least, I would like to express my gratefulness to my friends and parents for their continuous support and encouragement. Special thanks to my beloved parents for the immense love and encouragement throughout this study.

Table of Contents

List of Figures

List of Schemes

List of Tables

1.0 Introduction

1.1 Cellulose

Cellulose, the most abundant natural biopolymers in the world, can be produced from many natural resources including cotton, wood and sugar beets. It is a natural macromolecule with numerous advantages, such as renewable, biodegradable, non-toxic and environmentally friendly.

The repeatable units of cellulose are the anhydro-D-glucose linked by β-1, 4 glycosidic linkages (Figure 1). The glucose is a six-carbon ring unit connected by a single oxygen between two carbons. Each anhydroglucose unit possesses three hydroxyl groups which can react with many other functional groups. The polymerization degree can approach 20 000, depending on source of the celluloses[1-3]. Cellulose is very stable, and this is attributed not only to the backbones of the glucose chains, but also due to the intra-chain hydrogen bondings between hydroxyl groups and oxygen between the glucose units. It is important to know the structure of cellulose as it offers the explanations for its characteristic properties, such as hydrophilicity, chirality, and high functionality.
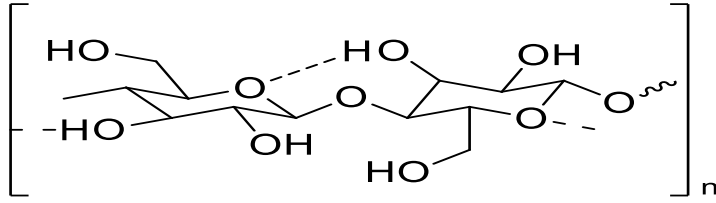
Figure 1. The chemical structure of cellulose.

1.2 Cellulose nanocrystal (CNC)

Cellulose nanocrystals (CNCs) are products from acid hydrolysis of native cellulose fibers with a rod-shaped nanoscale structure[4]. The diameter of CNC is 1 to 20 nm while the length of CNC is 200 to 500 nm. Also, different derivations of natural cellulose produce different morphologies in the cellulose nanocrystal (Figure 2). Transmission electron microscopy (TEM), scanning electron microscopy (SEM) as well as atomic force microscopy (AFM) are widely used to study the morphologies of cellulose. The diagram (Figure 2) shows that the length of crystallites from tunicates is in micrometers while the length of crystallites from wood and cotton is much shorter, around several hundred nanometers. This difference is mainly due to the fact that tunicate cellulose is highly crystalline, and only a small fraction of amorphous regions are being cleaved[9].

Compared with natural cellulose, CNC is a kind of material with exceptional strength and physicochemical characteristics, such as nanoscale dimension, high surface area, high specific modulus and many other unique properties[5-7]. Due to its advantages, various types of chemical modifications on the surface of CNC were

2

performed to achieve different applications. Currently, CNC has been used in enzyme immobilization, catalyst, antimicrobial medical applications and drug delivery.[8].
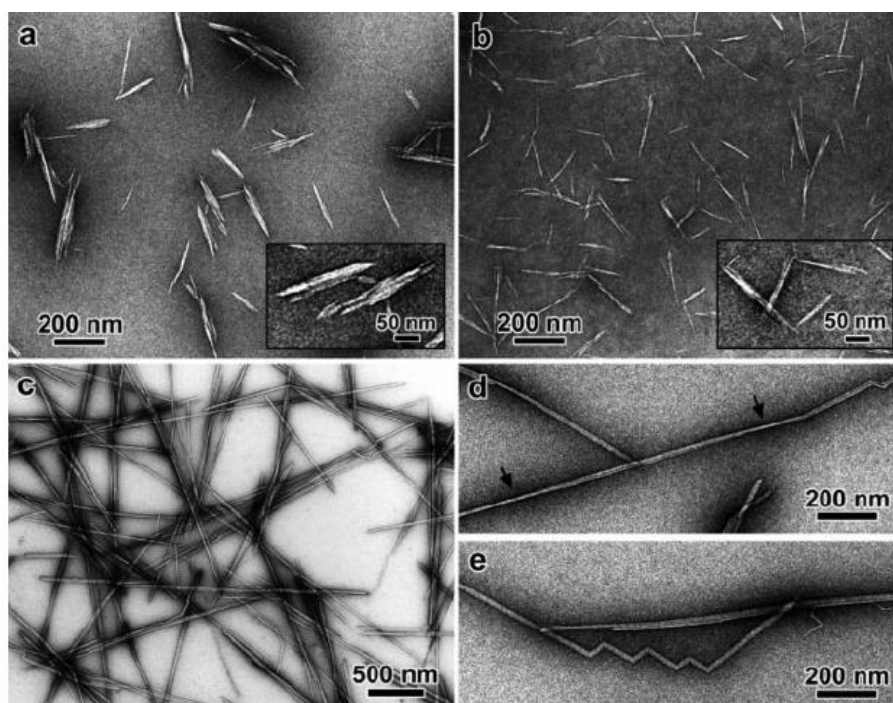
Figure 2. TEM micrographs of nanocrystals obtained by sulfuric acid hydrolysis of (a) cotton (b) avicel (c-e) tunicate cellulose[9].

1.2.1 Preparation of cellulose nanocrystal

The main process to produce CNC is acid hydrolysis. Cellulose contains both amorphous regions (to make materials flexible) and crystalline regions (to ensure the stability of CNC). The crystalline regions are highly ordered with the parallel stacking structures due to van der Waals forces and intermolecular hydrogen bonding[10]. Acid hydrolysis was used to remove the amorphous regions while the highly crystalline domains remained intact due to the strong interactions within its structures. If the hydrolysis of amorphous region is incomplete, the crystallinity will decrease. In this

case, the tensile strength, stiffness and many other properties will be affected. However, the aspect ratio will also be reduced due to too much hydrolysis[11-12].

The characteristics of the final materials can be influenced by many conditions, such as cellulose sources, reaction time, temperature and the acid[9]. Beck-Candanedo et al. (2005) found that the most important parameter is the reaction time during acid hydrolysis. The length of nanocrytals becomes shorter by increasing the hydrolysis time[11]. However, cellulose chains are hydrolyzed into anhydroglucose units if the reaction time is too long[13]. Also, high temperature and acid concentration have the same effects as the reaction time in the hydrolysis process. Shorter nanocrystals are produced when the temperature is high[15].
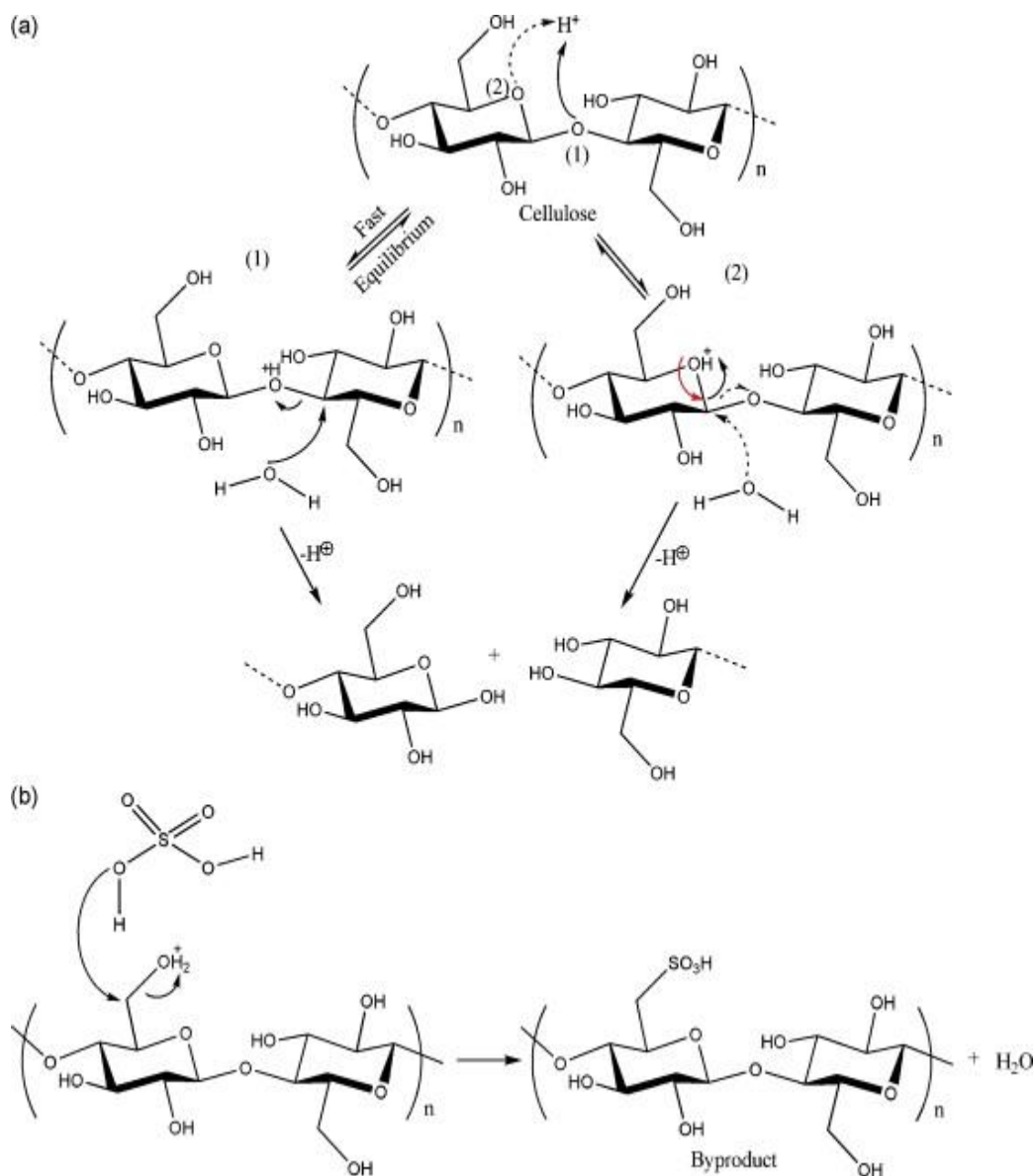
Figure 3. (a) Acid hydrolysis mechanism, (b) esterification of cellulose nanocrystal surface[16].

In acid hydrolysis, sulfuric acid and hydrochloric acid are extensively used for CNC production. However, phosphoric and hydrobromic acid have also been reported for hydrolysis[17]. Figure 3 shows that the process of hydrolysis of CNC involves the protonation of the glycosidic oxygen or the cyclic oxygen by protons in the acid[18]. The amorphous domains will be disrupted and the shorter chains of cellulose will be

achieved due to the additional water. At the same time, the backbone of the cellulose chains consisting of the rod-like rigid crystallites with high mechanical strength will be preserved. The hydroxyl groups on the surface of CNC can also react with sulfuric acid to yield new sulfate ester groups, which introduce more negative charges on the surface of CNC (Figure 1.3b). The electrostatic repulsion between anionic sulfate groups assures the dispersity of CNC in aqueous as well as some organic solutions, such as alcohol, dimethylformamide and dimethyl sulfoxide16. However, hydrolysis in hydrochloric acid will lead to flocculation of CNC in aqueous solution[19].

Overall, cellulose nanocrystals have higher surface area and aspect ratio than pristine cellulose, which is important for drug delivery system. Besides, the negatively charged sulfate groups can bind with many cationic drugs via electrostatic interaction. The numerous hydroxyl groups on the surface of CNC can also be modified to react with functional groups and polymers that can be used for drug loading and release.

1.2.1 Properties of cellulose nanocrystal

Due to the rigid rod-shape structure after acid or enzyme hydrolysis, CNC becomes one of the strongest and stiffest natural materials with exceptional properties, for example, high tensile strength (7500 MPa), high stiffness (Young's modulus of 100－140 GPa), high aspect ratio (70) and large surface area (150－250

m^2 /g)[8]. What is more, the crystalline regions of CNC are considered to be gas impermeable due to strong interfibrillar bonds between CNC nanofibers. The two main effects of film oxygen permeability are density and porosity of the CNC film.

Besides its remarkable strength and physicochemical properties, CNC is also non-toxic and environmental friendly. CNC displays no significant effects or cytotoxicity on mouse or human macrophages[7]. As a result, CNC is widely used in many biocomposite applications, such as enzyme immobilization, antimicrobial and medical materials[20].

1.3 Chemical Modifications of CNC

CNC has a tendency to aggregate in different environments because of its small size and large surface area. In order to increase the stability of CNC in solutions for the desired applications, chemical modifications of CNC have been carried out on the hydroxyl groups on the surface of CNC. However, in each anhydroglucose with three hydroxyl groups, the chemical reactions can only be conducted on the primary hydroxyl group which is connected with –CH$_2$- group. Various modifications, such as sulfonation, oxidation[20], cationization[21], silylation[22], and grafting via acid chlorides[23], acid anhydrides[24] or isocyanates[25] have been reported (Figure 4).
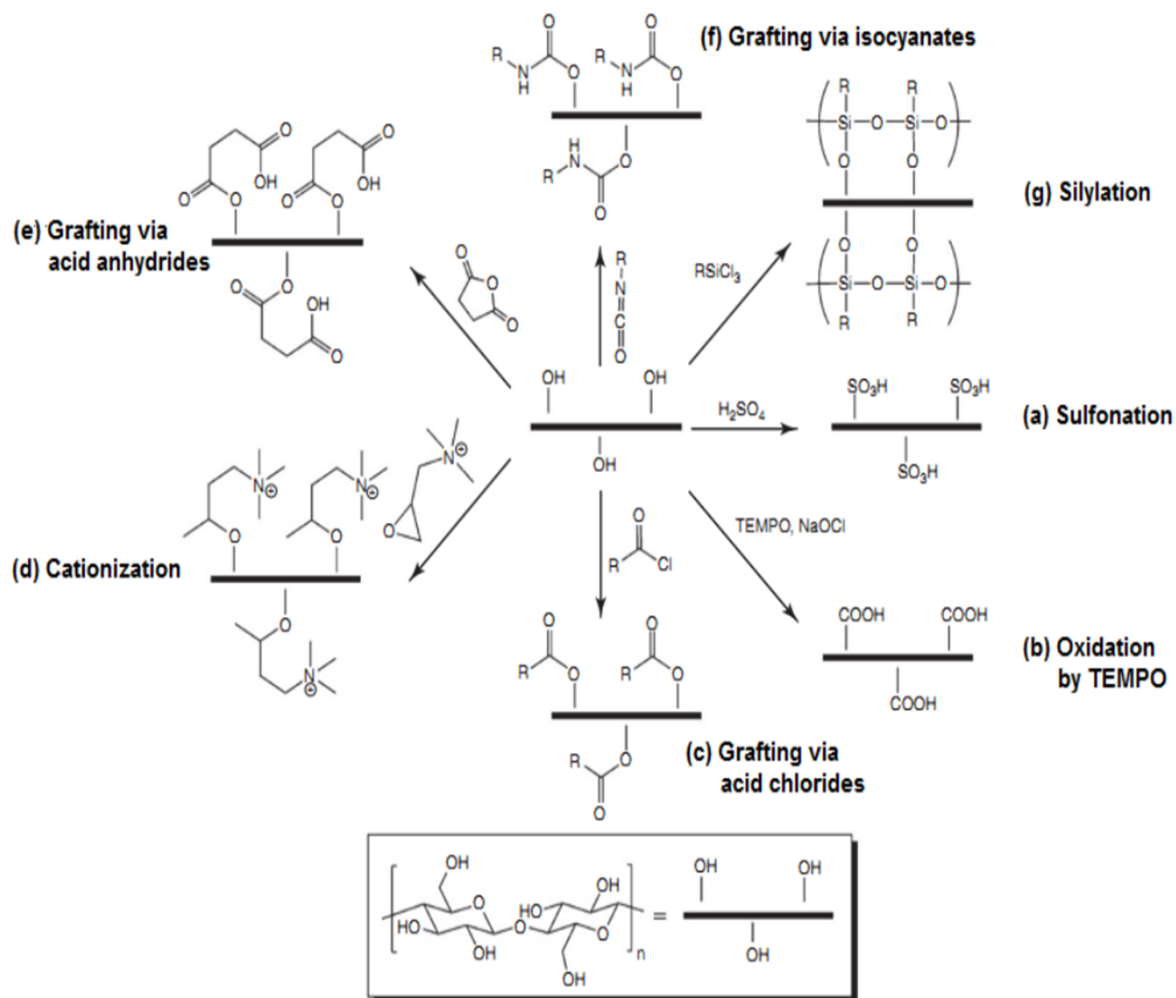
Figure 4. Various modifications of CNC[20-25]. Figure adapted from reference[26].

1.3.1 TEMPO Oxidation

TEMPO (2, 2, 6, 6-Tetramethylpiperidine-1-oxyl radical) is considered to be one of the most representative reagents in the CNC oxidation. In this reaction, the primary hydroxyl group on the surface of CNC was oxidized by NaClO with catalytic amounts of TEMPO and NaBr to carboxylic groups while the secondary hydroxyl groups remained intact[27].

This experiment was carried out in an aqueous solution at pH 10-11 to avoid

destroying the structure of CNC. The oxidization can be controlled stepwise by

controlling the addition of the amounts of NaClO or reaction time. The oxidation

degree will be higher with larger amounts of NaClO or longer reaction time.

Conductometric titration was used to measure the concentration of carboxylic

groups to identify the degree of oxidation. The oxidized products can also be

analyzed by nuclear magnetic resonance (NMR). Figure 5 shows the oxidation

procedure of polysaccharides primary hydroxyl groups to carboxyl groups by the

TEMPO-mediated oxidation. Tempo modified CNC shows a very good dispersion in

polar solvents.
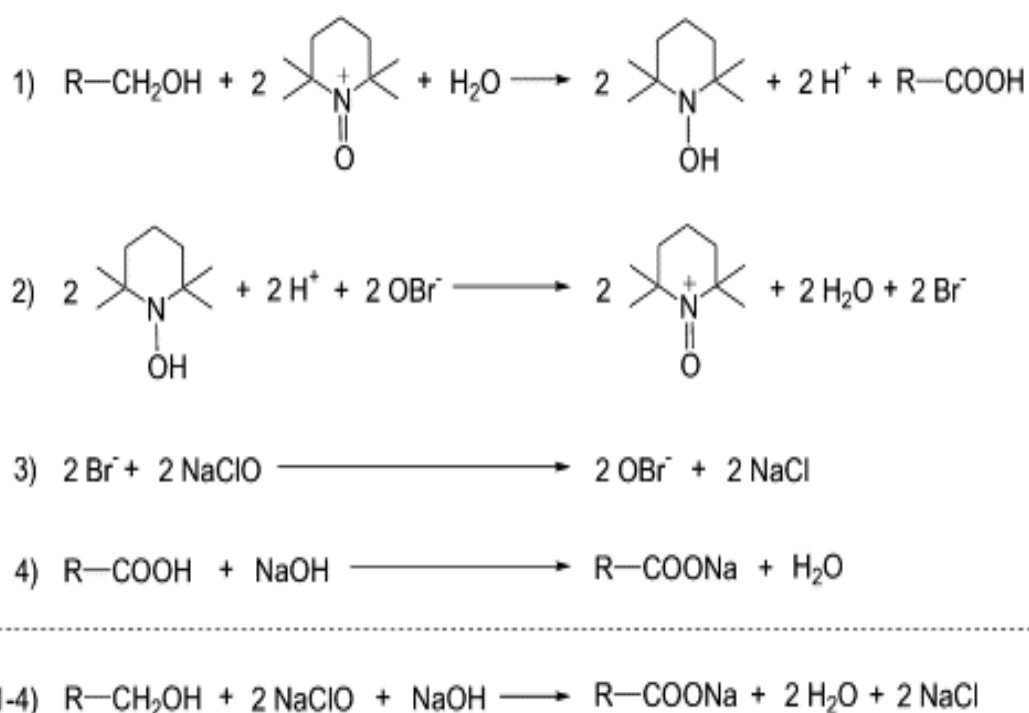
Scheme 1. Formulae for oxidation of primary hydroxyl groups of polysaccharides to carboxyl

groups by the TEMPO-mediated oxidation[27].

1.3.2 GTMAC CNC

GTMAC grafting of CNC is under alkaline conditions, water as a catalyst in organic solvent, through filtration glyceryl trimethyl ammonium chloride (GTMAC) of epoxy ethane in open loop function reacting with active hydroxyl groups on the surface of the CNC. Fourier Transform Infrared Spectroscopy (FTIR) was used to confirm the presence of cationic GTMAC on the surface of CNC.

It is found that the zeta-potential of GTMAC-CNC is around +30±5mV, compared to -39±3mV of pristine CNC, indicating a reversed surface charge after modification. This cationically modified CNC was well-dispersed and stable in aqueous media due to enhanced cationic surface charge density[28]. The reaction parameters, such as water content, reaction molar ratio and the reaction media are very important in controlling the surface charge density of CNC.
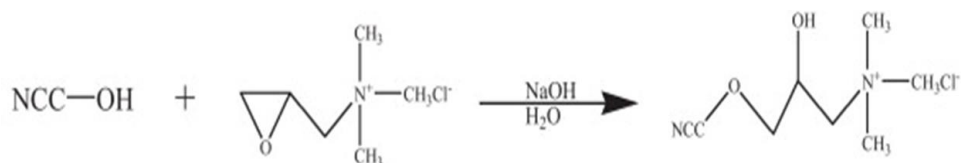
a) Step 1. Desired reaction: Cationization of CNC
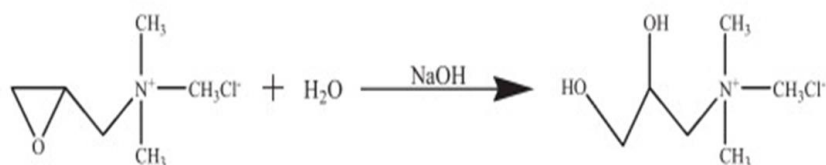
b) Step 2. Side reaction: Hydrolysis of GTMAC.
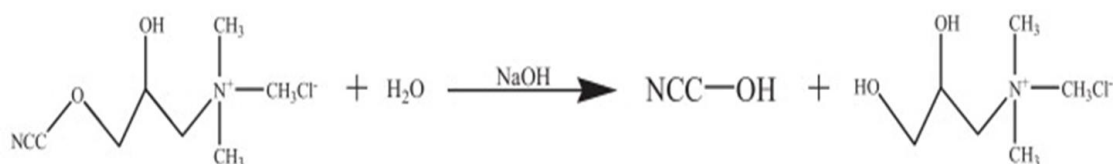
c) Step 3. Side reaction: Degradation of cationic CNC

Scheme 2. Competitive reactions during the cationic modification of NCC using GTMAC/H2O/NaOH

System[28].

Scheme 2 shows GTMAC is consumed in a competition between the two

reactions during cationization: cationization of NCC (Scheme 2a), which is beneficial,

and the GTMAC hydrolysis reaction (Scheme 2b), which should be avoided as much

as possible. It is easy to conclude that too much water will lead to the hydrolysis of

GTMAC. As a result, the cationization efficiency of reaction will be reduced.

Therefore, the water content of the reaction system should be carefully controlled in

the cationization process. The optimum water content was found to be 36 wt% for

aqueous based media and 0.5 water to DMSO volume ratio for aqueous-organic

solvent reaction media[28].

1.3.3 Grafting polymers

Grafting polymers on the surface of CNC is an effective way to increase the stability and dispersity of CNC in aqueous and organic suspensions. There are two main methods for grafting polymers, grafting-to, which involves the reaction between the functional groups of pre-synthesized polymer chains and hydroxyl groups on the CNC surface, and grafting-from, which is the surface initiated, in-situ polymerization. Grafting-to method includes grafting polycaprolactone (PCL) with various molecular weights[29], amine-functionalized PEG[30], DNA oligomers[31], etc. Grafting-from method means that polymers are grown from surface-immobilized initiators which are the primary hydroxyl groups on the surface of CNC. Ring-opening polymerization[29], microwave irradiation[32] and in-situ solvent exchange[33] are the typical examples for grafting-from polymerization.

(PLS CHECK ALL YOUR FIGURE NUMBERING!!)

1.4 Applications of CNC

As one of the most abundant natural biopolymers in the world, CNC has been envisioned for many useful applications due to its distinctive properties. The main application of CNC is to reinforce the polymeric matrix in nanocomposite materials. The use of CNC as reinforcing fillers in poly (styrene-co-butyl acrylae)

(poly(S-co-BuA))-based nanocomposites was first reported by Favier in 1995[34]. Since

then, many researchers have designed new nanocomposite materials by

incorporating CNC into a wide range of polymeric matrices. As a result, diverse

unique applications have been explored in different fields including pharmaceutical

tablets and food additives, such as stabilizers, texturing agents and fat replacers. The

lithium battery products with CNC as a mechanical reinforcing agent for

low-thickness polymer electrolytes have also been developed[35]. What is more, CNC

can also be used in security paper because of its liquid crystal property. The hydroxyl

groups on the surface of CNC can also be further modified to obtain functionalized

CNC for diverse applications.

1.4.1 CNC in drug delivery

Besides the mechanical and chiral nematic liquid properties of CNC, it is also

safe, non-toxic and biodegradable. Applications in biomedical fields have attracted

increasing attention. CNC is a renewable biopolymer which can be used as

protein/enzyme carriers, catalysts, and biosensors/bioimaging and drug delivery.

Various drug delivery systems including liposomes, micelles and microgels have been

developed and studied by researchers.

Microcrystalline cellulose was often blended with other pharmaceutical

excipients to form drug-loaded tablets for oral drug administration in the medical

industry. Derivative cellulose including carboxymethyl cellulose (CMC), ethyl cellulose,

and methyl cellulose have also been applied in topical, oral and injectable formulations.

In addition, CNC has been considered as one of the potential nanomaterials for targeted drug delivery due to its exceptional physical properties suitable for internalization within the cell. The hydroxyl groups on the surface of CNC can react with hydrophobic or nonionized drugs after modification. Numerous trials have confirmed that CNC is non-toxic and environmental friendly. Scientists found that ionizable drugs, such as tetracycline and doxorubicin that were bound to CNC could be released rapidly within one day.

1.5 Introduction of liposomes

Lipids, as well as proteins and nucleic acids are the three main essential biomolecules for the living system. Most lipids are natural molecules, such as fats, waxes, sterols and fat-soluble vitamins[34]. The main biological functions of lipids include energy storage, signaling, and structural components of cell membranes. The amphiphilic lipids are the dominant components of biological membranes, along with spherical liposomes, which have been widely used as vehicles for drug delivery.

1.5.1 Structure of liposomes

Liposomes are made of one or more bilayers of phospholipid molecules with

self-assembling spherical structures (Figure 6). The liposomes with one bilayer separate the aqueous core from the outer aqueous solution. The size of liposomes ranges from 20nm to 10µm. When the size is from 100nm to 300nm, the liposomes display the best stability.

Liposomes can be prepared by disrupting biological membranes, which mainly refers to the glycerophospholipids (Figure 5). The polar part of lipids can either be charged (positively or negatively), zwitterionic or neutral. The reason for the formation of different structures by amphiphilic lipids is due to their duel preference for the solvent.
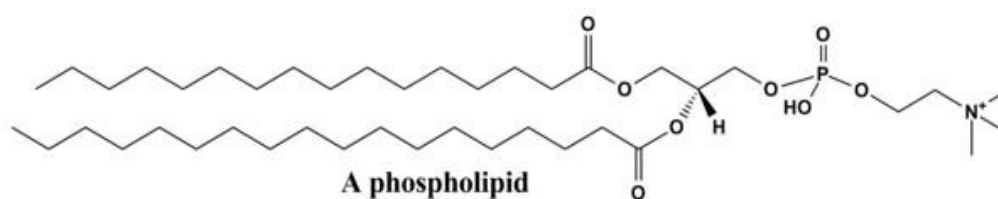
Figure 5. Chemical structure of phosphatidylcholine.
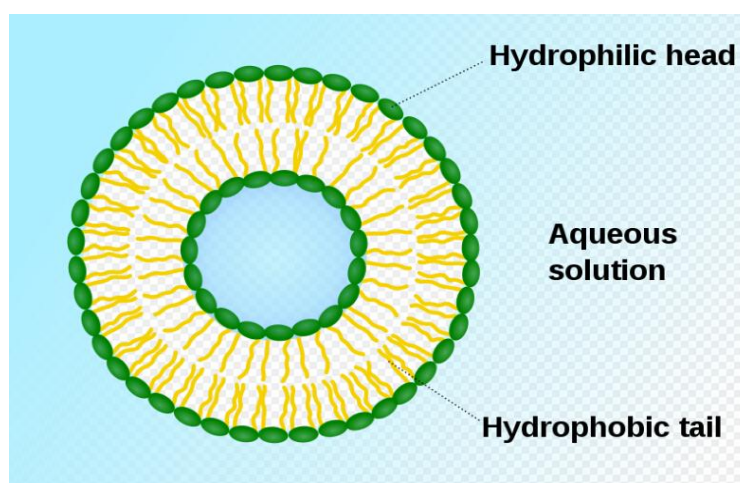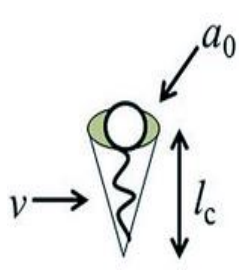
Figure 6. Scheme of a liposome formed by phospholipids in an aqueous solution[35].

15

In water solution, the amphiphiles dissolve as monomers first. Then the polar

heads of lipids have a tendency to align towards the polar aqueous environment

while hydrophobic parts are expelled from the aqueous solution and sequestered

within the interior of the aggregate. This kind of aggregation is determined not only

by the concentration of lipids, but also the packing parameters of the amphiphile.

Table 1 shows the different aggregate structures depending on the surfactant packing

parameter S, which is defined by: S= $\frac{v}{a*l}$. In this equation, v refers to the volume of

the hydrophobic portion of the amphiphile, l is the length of the hydrocarbon chains

and a is the effective area per head group. When the packing parameter is lower

than one-third, the lipids possess a cone-like shape and will pack together to form

spherical micelles. When the S is in the range of 1/2 to 1, the lipids appear to have a

cylindrical shape and pack together to from bilayer in an aqueous environment (Table

1). Most of the lipids have a tendency to form the bilayer structure.

		Critical Packing Parameter $(v/a_0 l_c)$	Critical Packing Shape	Structures Formed

Critical Packing Parameter (v/a_0l_c) | Critical Packing Shape | Structures Formed

< 1/3   Cone   Spherical micelles

1/3 – 1/2   Truncated cone   Cylindrical micelles

1/2 -1   Truncated cone   Flexible bilayers, vesicles

~1   Cylinder   Planar bilayers

>1   Inverted truncated cone or wedge   Inverted micelles

$$CPP = v/a_0 l_c$$

Table 1. Different packing structures as a function of the surfactant packing parameter S[36].

1.5.2 Preparation of liposomes

In order to obtain different kinds of liposomes with unique applications, a number of methods for preparing liposomes have been designed. The three main

parameters of liposomes are size, lamellarity and the homogeneity of the liposomal suspension.

One way to prepare liposomes is the gentle hydration method. Phospholipids are distributed in a thin film on the surface of glassware by dissolving the phospholipids in an organic solvent, like chloroform, and later evaporating the solvent[37]. However, the extrusion method has been widely used in recent years. Liposomes are extruded through a polycarbonate filter under pressure in order to create a homogenous size distribution. When the size of liposomes are between 100-200nm, liposomes can load drugs in the cells without inducing an immune response[38]. In addition, there are many other novel methods of making liposomes, such as sonication and ethanol injection methods.

1.5.3 Liposomes in drug delivery

Liposomes are one of the most tested and versatile systems in drug delivery due to the following advantages. First, liposomes are safe and tolerated. Many liposome-based anti-cancer and anti-infection drugs have been extensively used indicating the nontoxicity of liposomes. Second, low reactogenicity has been approved by numerous human trials of liposomal vaccine candidates. Third, liposomes are known to be completely biodegradable as they are often composed of lipids that occur naturally in cell membranes. What is more, many types of antigens, such as peptides, proteins, and nucleic acids, can be incorporated in liposome

formulations with appropriate modification, which shows the versatility of the liposomes.
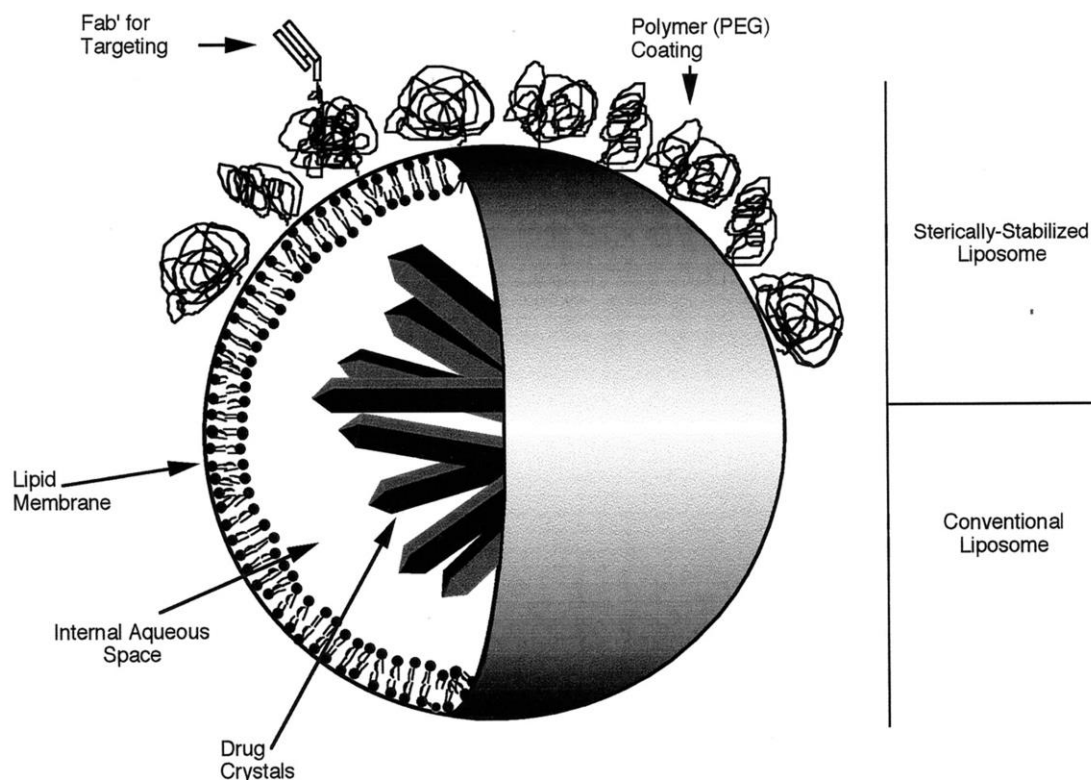
Figure 7. Structure of conventional and sterically-stabilized liposome[38].

Liposomes have been successfully used as drug carriers because they can transport many different types of drugs at high concentrations. Both hydrophilic drugs and hydrophobic drugs can be loaded into liposomes due to their superior structure. Hydrophilic and amphiphilic drugs can be encapsulated into the aqueous core while hydrophobic drugs can be incorporated into the lipid bilayer (Figure 7). The sizes of liposomes used for drug delivery are in the average range of 50 to 200nm.

Liposomes are divided into two types according to their composition, and the mode of stabilization, i.e. conventional or sterically stabilized liposomes. Conventional liposomes are made of simple lipid bilayers containing high phosphatidylcholine (PC) and cholesterol moieties. Sterically stabilized liposomes are lipid bilayers possessing either a ganglioside GM1 or synthetic neutral polymer polyethylene glycol (PEG) [39]. This kind of liposome is more stable because they can reduce the binding of serum opsonins and minimize their interaction with the reticuloendothelium system (RES) [40]. As a result, sterically stabilized liposomes remain in circulation for a longer time, allowing the exploitation of leaky tumor vasculature and increasing the blood flow to the tumor, which is known as the enhanced permeability and retention (EPR) effects.

In order to deliver liposome-encapsulated drug into specific sites in human bodies, liposomes are always designed with temperature- or pH-sensitive properties. The basic idea is that the liposomal membrane will reorganise due to environmental changes. In this case, the encapsulated drugs can be released. For example, internalized DOPE-based pH-sensitive liposomes can deliver hydrophilic substances to the cytosol of target cells[41].

Nowadays, liposomes have been approved to deliver many kinds of drugs and anti-cancer agents, such as doxorubicin (Doxil) and daunorubicin (DaunoXome). In addition, new methods for the efficient delivery of drugs into the inner ear have

been developed, making a significant contribution to the treatment of cochlear diseases or injury and the amelioration of hearing loss. The size of liposome is of great importance in overcoming various in-vivo barriers for systemic delivery such as blood components, reticuloendothelial system uptake, tumor access, extracellular matrix components, and intracellular barriers[42].

1.6 Surface interaction

It is of great importance to understand the surface interaction in many fields, such as biological and chemical coatings, elucidation of the mechanisms and the structure and composition of the implant interface. There are varieties of interactions between different surfaces. However, the three main kinds of surface interactions are electrostatic interaction, covalent linkage, and hydrogen bonding. For example, the interaction between cationic liposomes with negatively charged graphene oxide is electrostatic interaction[43]. Carbon nanotubes were combined with liposomes by covalent bonding[44]. The interaction between nanodiamond and liposomes is hydrogen bonding[45].

1.6.1 Electrostatic interaction

The electrostatic interaction appears in two particles with different charges (either positive or negative) by a finite distance. The ionization or attachment of ionic species is the main reason to this interaction. Coulomb's law is normally used to

describe the strength of electrostatic interactions, for example, the repulsive forces between similar charges and the attractive forces between opposite charges. The forces are determined not only by the particle charges, but also the distance between two particles.

In solids or solutions, there will be screening effect which reduces the electrostatic field and Coulomb potential of the ion. As a result, the electrostatic interaction can be completely eliminated by increasing the salt content.

1.6.2 Covalent linkage

The covalent bond is formed between two atoms sharing one or more electron pairs. In most cases, each atom of the molecules will have a stable electronic configuration by sharing electrons to attain the equivalent of a full outer shell. For example, in water molecules, there is a covalent bond between oxygen and hydrogen. Each of the covalent bonds contains two electrons - one from a hydrogen atom and one from the oxygen atom. So the outermost electrons of hydrogen are 2 while the oxygen is 8, which is stable for both atoms.

There are many kinds of interactions in covalent bonding, such as σ-bonding, π-bonding, metal-to-metal bonding and agnostic interactions. The covalent leakage is influenced by the connected atoms. If the two atoms have equal electronegativity, the covalent bond will be non-polar (H-H). The unequal electronegativity leads to a polar covalent bond (H-Cl).

1.6.3 Hydrogen bond

A hydrogen bond is a special kind of interaction, which is known as electrostatic attraction between a hydrogen (H) atom and a highly electronegative atom such as nitrogen (N), oxygen (O) or fluorine (F). It is often described as a strong dipole-dipole attraction instead of a truly covalent bond.

The hydrogen bond can occur either intermolecular (between molecules) or intramolecular (within different parts of a single molecule). The strength of hydrogen bond is stronger than a van der Waals interaction, but weaker than covalent or ionic bonds. This type of bond can occur in inorganic molecules such as water and in organic molecules like DNA and proteins. An example of this is how the hydrogen bonds in water strengthen the interactions between molecules giving water a higher boiling point then other group 16 hydrides. The length of hydrogen bond can be determined by many parameters, such as bond strength, temperature, and pressure.

2.0 Experimental procedures

2.1 Liposome

The names and structures of the three kinds of lipids used in this thesis are shown in Figure 1. DOPC= 1, 2-dioleoyl-sn-glycero-3-phosphocholine; DOTAP = 1, 2-dioleoyl-3-trimethyl ammonium-propane; DOPG = 1, 2-dioleoyl-sn-glycero-3-phospho-(1'-rac-glycerol) (sodium salt); Rh-PE = 2-dioleoyl-sn-glycero-3-phosphoethanolamine-N-(lissaminerhodame B sulfonyl) (ammonium salt). 1 % Rh-PE was used to label the liposomes.
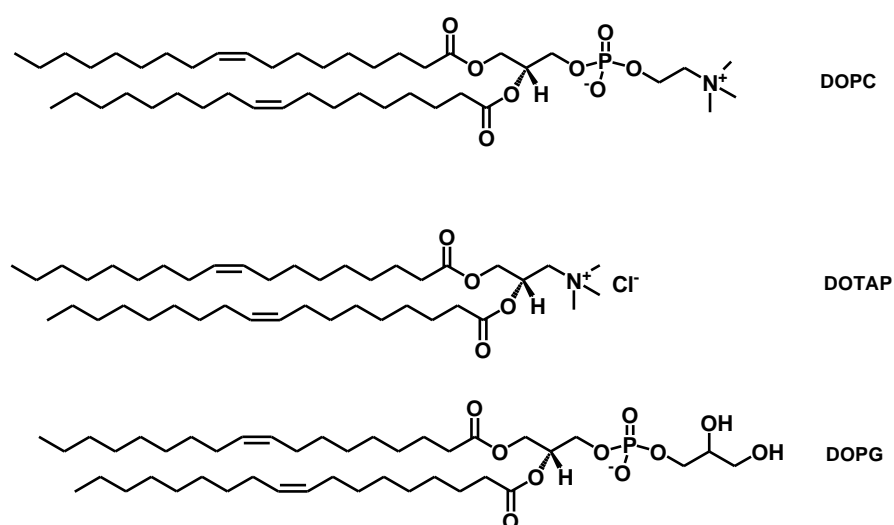
Figure 8. Names and structures of the lipids used.

2.2 Materials

The hydrolyzed cellulose nanocrystals (average charge density is 0.26 mmol/g) were supplied by CelluForce Inc. All the phospholipids were purchased from Avanti

Polar Lipids. Sodium phosphate, 4-(2-hydroxyethyl)-1-piperazineethanesulfonic acid

(HEPES), sodium acetate and sodium nitrate were purchased from Mandel Scientific

(Guelph, Ontario, Canada). MilliQ water was used for preparing all the solutions and

buffers. All the reagents were purchased from Sigma-Aldrich unless otherwise stated.

2.3 Preparation of liposomes

The standard extrusion method was used to prepare liposomes. The

mini-extruder was purchased from Avanti Polar Lipids. DOPC, DOPG and DOTAP (a

total mass of 2.5 mg) were dissolved in chloroform respectively. 1 % Rh-PE was mixed

with different kinds of lipids in chloroform to prepare Rh-labeled liposomes.

Chloroform was removed under a N_2 flow. Subsequently, the samples were stored in

a vacuum oven overnight at room temperature to remove trace amount of residual

chloroform. The dried lipids were stored at -20 ℃ under a N_2 circumstance prior to

use. To prepare liposomes, the lipids were first dissolved in 0.5 mL buffer A (100 mM

NaCl, 20 mM HEPES, pH 7.6) and put in the ultrasonication bath occasionally to get a

well-dispersed solution. Next, lipids were extruded through two stacked

polycarbonate membranes (pore size = 100 nm) twenty-one times. The final solution

was transparent after extrusion, which indicates downsize of the lipid structures and

formation of liposomes.

2.4 TEMPO mediated oxidation of CNC

TEMPO is considered to be one of the most representative oxidation reagents in

the CNC oxidation. In this experiment, the primary hydroxyl groups on the surface of

CNC were oxidized by NaClO in water. A homogenous solution of 1 % CNC (100 g) was

made with sonication. Then, TEMPO (3.85 mg, 0.0246 mmol) and NaBr (50.8 g,

0.4928 mmol) were added to CNC suspension using an ice bath at 5 ℃. The solution

was adjusted to pH 10 by adding 0.5 M NaOH. A total amount of 6 mL NaClO (6.15 %)

was added into solution gradually over 30 minutes while the pH was maintained at

10 by adding NaOH under agitation (TEMPO oxidation) (Scheme 3).

After 4 hours reaction, the pH of the solution was kept at 10, suggesting the end of

oxidation. Ethanol was used to precipitate the oxidized products. In order to get a

purified sample, the solution was dialyzed for at least 2 days in MilliQ water.
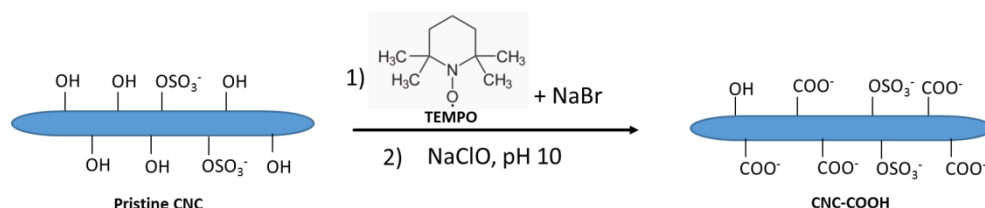
Scheme 3. Scheme of TEMPO oxidation for pristine CNC.

2.5 Desulfation of CNC

The sulfate ester groups of CNC were removed by hydrolysis under basic

conditions prior to functionalization with glycidyltrimethylammonium chloride

(GTMAC). In a typical procedure, 50 mL CNC dispersion (2 % ww) was mixed with 30

mL NaOH (5 M). The mixture was heated at 65 ℃ for 5 h with stirring. After cooling

down to room temperature, the mixture was diluted with 100 mL MilliQ water and

dialyzed against water for 3 days. The suspension was then allowed to stand for one

hour, CNC settled down to bottom and left clear supernatant. The supernatant was

decanted, and the suspension was concentrated by evaporation at reduced pressure.

The concentrated sample was finally freeze dried.

2.6 Preparation of GTMAC grafted CNC

Desulfated CNC (0.5 g) was dispersed in 50 mL DMSO using homogenizer. To

this dispersion, 0.48 g (3.0 mmol) GTMAC and 0.5 g (0.6 mmol) TBA•30H$_2$O were

added. The mixture was heated at 65 ℃ for 5 h (Scheme 4). This reaction involves a

nucleophilic reaction between the alkali activated hydroxyl group of CNC and epoxy

group of GTMAC. In addition, this reaction was carried out in DMSO instead of water

to avoid hydrolysis of ester groups at basic condition in aqueous media (Scheme

5).The reaction was then allowed to cool down to room temperature. Upon cooling,

the mixture was diluted with 100 mL MilliQ H$_2$O and dialyzed against MilliQ water for

seven days to remove unreacted GTMAC and DMSO. After dialysis, the concentration

of CNC-GTMAC was determined gravimetrically.
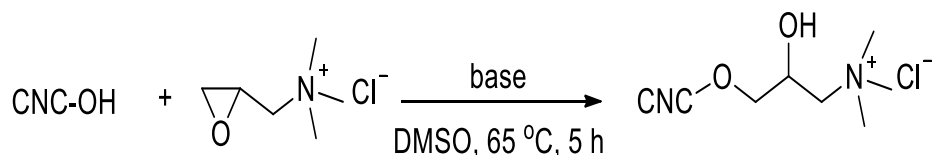
Scheme 4. The reaction of CNC and GTMAC.

Hydrolysis of GTMAC
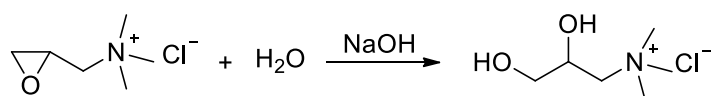
Hydrolysis of CNC-GTMAC
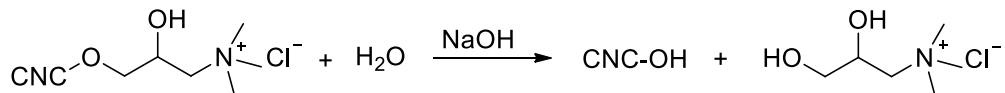
Scheme 5. The hydrolysis of GTMAC and CNC-GTMAC in aqueous media under basic condition.

2.7 Characterization of TEMPO CNC
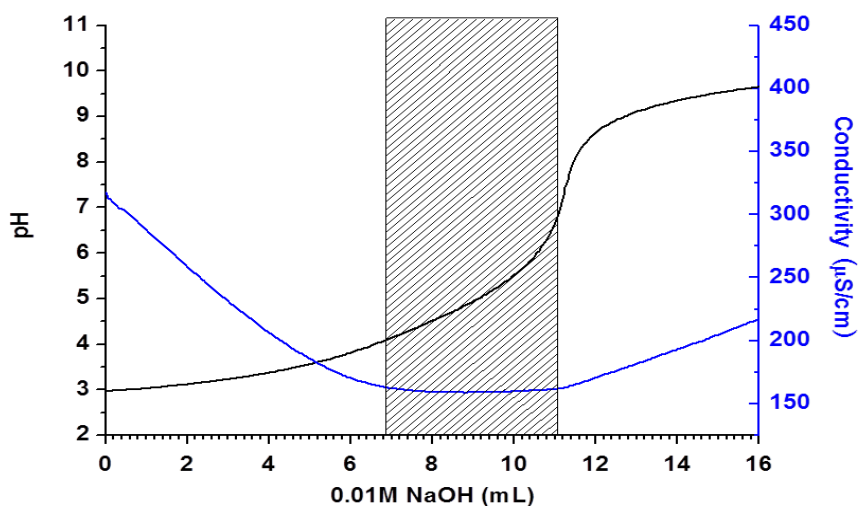
Figure 9. Potentiometeric and conductometric titration of TEMPO CNC.

In order to calculate the content of carboxyl groups on the surface of TEMPO CNC, a Metrohm 809 autotitrator was used for titration. 40 mg TEMPO CNC was dispersed in MilliQ water. The pH of suspension was adjusted to 3 by adding 0.1 M HCl. Then, 0.01 M NaOH was titrated into suspension until the pH was 10 under stirring. The pH and conductivity of suspension could be monitored on the screen. The volume of

NaOH was used to calculate the amount of carboxylic functional groups on TEMPO CNC (Figure 9). We can see that 4.2 ml 0.01 M NaOH was consumed and the -COOH content in TEMPO CNC was 0.91 mmol/g (COOH/CNC) (14.6 %).

2.8 Characterization of GTMAC CNC

The successful cationization of CNC was confirmed using zeta-potential measurement and the content of GTMAC on CNC was determined by conductomatric titration using $AgNO_3$. The zeta-potential of the CNC suspension changed from -40 mV before modification to 32.1 mV after cationization. This value shows that the cationic CNC is able to give a stable suspension. The trimethylammonium chloride content was determined by conductometric titration using $AgNO_3$ aqueous solution as titrant. Typically, 40 mg CNC-GTMAC in 50 mL MilliQ H_2O was titrated using 0.01 M $AgNO_3$ (aq). The content of trimethylammonium chloride was found to be 0.09 mmol/g CNC (Figure 10).
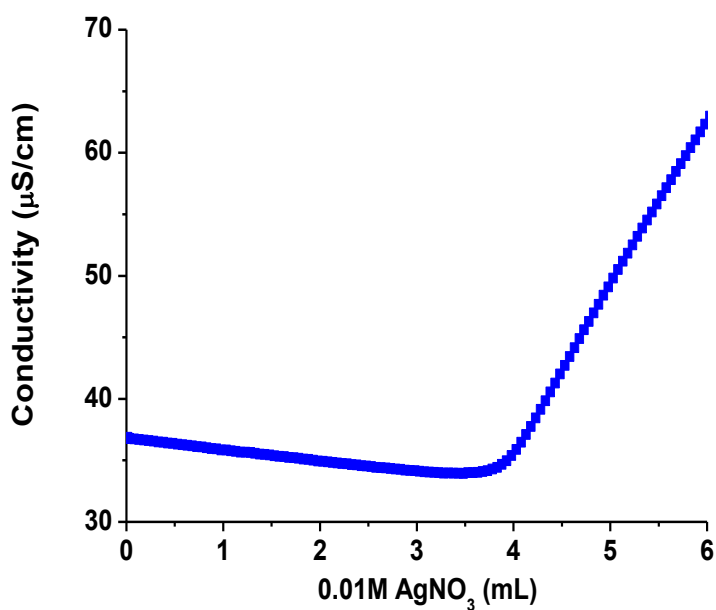
Figure 10. Conductometric titration of 40 mg CNC-GTMAC with 0.01 M AgNO$_3$ aqueous solution.

2.9 pH-dependent studies

0.1 mg/ml CNC stock was prepared by dissolving CNC in 10 mM phosphate buffer with pH value from 3 to 8. Then, 1 μL 5 mg/ml DOPC, DOPG and DOTAP liposomes (with 1 % Rh-PE labeled) were mixed with CNC stock, respectively. Afterwards, the CNC-liposome conjugation and free liposomes were separated by centrifugation at 15000 rpm for 10 min. In this case, the conjugation of CNC and liposome could be spun down and the free liposomes were in the supernatant. The fluorescence intensity of the supernatant was measured to help calculate the adsorption of liposome.

2.10 Salt-dependent studies

0.1 mg/ml CNC was prepared by dissolving CNC in 10 mM phosphate buffer (pH 7) containing various NaCl concentration from 0 mM to 1670 mM. 1µL 5 mg/ml DOPC, DOPG, DOTAP liposomes were mixed respectively with prepared solution and then centrifuged at 15000 rpm for 10 minutes. The fluorescence of the supernatant was measured to figure out the adsorption of liposome.

2.11 Liposome/CNC complex studied by DLS

To study the size of complexes formed between liposome and CNC, a dynamic light scattering (DLS) test was carried out. In a typical experiment, DOTAP, DOPG or DOTAP liposome with a concentration of 0.05 mg/ml was respectively mixed with 0.1 mg/ml pristine CNC, TEMPO CNC or GTMAC CNC from pH 3 to 8. After 10 min incubation, the size of the sample was measured by DLS (Zetasizer Nano 90, Malvern) at room temperature.

Zeta potential of 0.1 mg/ml pristine CNC, TEMPO CNC or GTMAC CNC, which was dispersed in 10 mM phosphate buffer from pH 3 to 8, was determined by DLS. In addition, the zeta potential test of 0.05 mg/ml DOTAP, DOPG or DOTAP in 10 mM phosphate buffer from pH 3 to 8, was also carried out on Zetasizer Nano 90, Malvern.

2.12 Calcein-loaded DOPC liposome leakage test

We do the leakage test for liposomes to study the biophysical effect of CNC on the liposomes. First, 5 µL Pd-10 column purified calcein-loaded DOPC was mixed with

595 µL HEPES (10 mM, pH 7.6) in a quartz cuvette. The whole solution was

monitored by fluorescence enhancement, of which the excitation wavelength was

485nm and the emission wavelength was 525 nm. After 5 min, 10 µL CNC (1 mg/mL)

was then added into solution. The fluorescence intensity was checked every 12

seconds. At 30 min, we added 10 µL 5 % Triton X-100 to terminate the test. A similar

experiment was carried out for DOPG.

2.13 Urea test

In order to find out whether the interaction between DOPC and pristine CNC

was hydrogen binding, we added urea into the solution to test the result. First, 1µL 5

mg/ml DOPC was mixed with 99µL 0 .1 mg/ml CNC in 10mM buffer at pH 3. Then,

the complexes were centrifuged at 15000 rpm for 10 min. After that, 10mM buffer at

pH 3 was used to wash the precipitates twice. Finally, we added 8M urea to incubate

the complex for 10 min. The solution was then checked under UV light compared

with the mixture between 1 µL 5 mg/ml DOPC and 99 µL 8 M urea without CNC.

3.0 Results and discussions

In recent years, carbohydrates have attracted great attention in nanotechnology because of their potential applications, such as drug delivery, imaging and sensing. Many researches have been carried out on CNC, one of the most abundant renewable and biodegradable nanomaterials. On the other hand, lipid-functionalized hybrid nanomaterials are extremely useful in drug delivery. Liposome, which is an ideal model for cell membrane, has been widely used in drug delivery systems. Their possibilities to enhance drug loading, improve bilayer stability and control content release have been shown in numerous papers[57].

However, little is known about the interaction between CNC and liposome, which is of great importance for the following reasons. In this way, further novel applications, for example, drug delivery vehicles, can be developed. In this thesis work, I studied fundamental interaction mechanism between CNC and liposome.

Fluorescence test is one of the most useful techniques in characterizing nanoparticulate delivery systems since it is highly sensitive and easy to prove and even quantify the adsorption between nanoparticles. Fluorophores, which can be located inside the cells or host system, have a selection of different wavelengths of excitation light. By using a fluorophore label, the fluorescence intensity was then measured to help calculate the adsorption efficiency. In this way, the adsorption between different nanomaterial systems can be detected by fluorescence techniques

no matter what kind of interaction, electrostatic interaction or hydrogen binding.
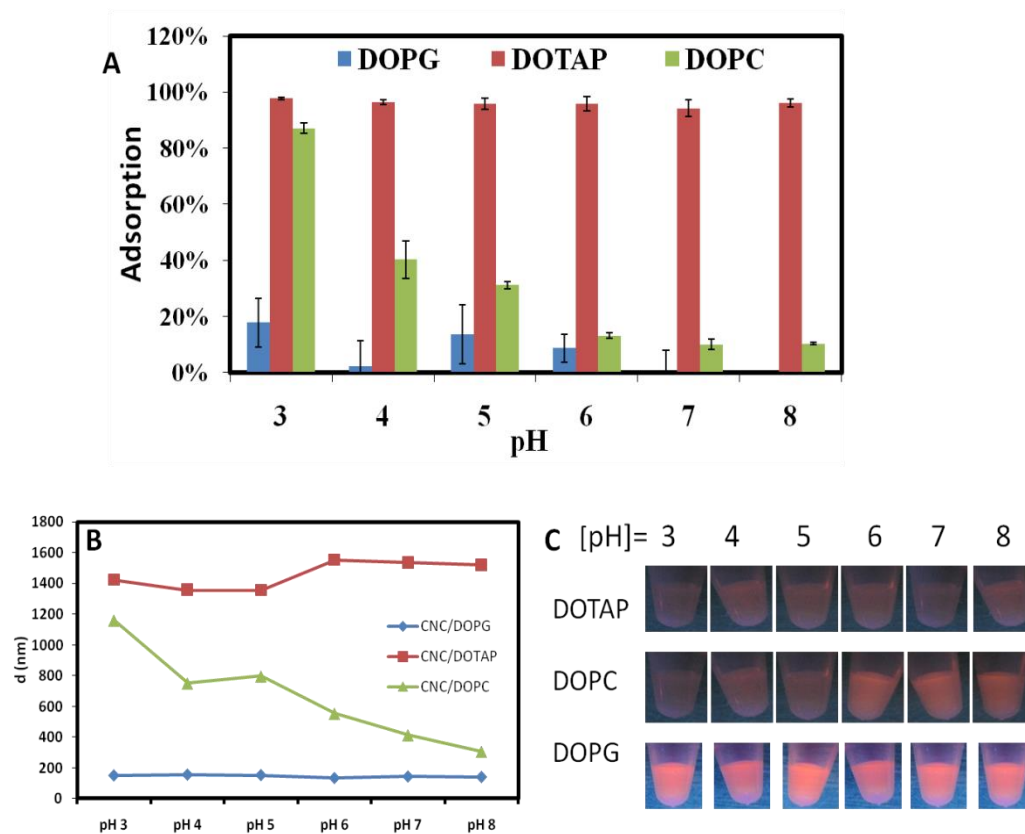
Pristine CNC

Figure 11. A) Adsorption of three types of liposomes by pristine CNC as a function of pH. B) Change of the complex sizes between pristine CNC and three types of liposomes as a function of pH. C) Photographs of Rh-labeled liposomes interacting with pristine CNC as a function of pH. High fluorescence indicates week interaction.

Zeta Potential(mV)	pH 3	pH 4	pH 5	pH 6	pH 7	pH 8
TEMPO CNC	-12.4	-29.6	-28.7	-29	-36.4	-29.1
Pristine CNC	-27.4	-27.6	-27.9	-28.5	-34.9	-34
GTMAC CNC	31.2	30.6	27.8	24.8	22.9	23.5

Table 2. Zeta-potential of different CNCs as a function of pH at 25℃

Zeta Potential(mV)	pH 3	pH 4	pH 5	pH 6	pH 7	pH 8
DOPG	-78.7	-80	-84.5	-85.3	-90.6	-88.2
DOPC	2.3	1.6	0.7	-1.3	-2.3	-3.4
DOTAP	28.4	26.3	25.3	23.2	22.5	19.8

Table 3. Zeta-potential of different liposomes as a function of pH

To have a systematic understanding, we tested a total of three types of CNC, carrying different surface groups. In order to test the adsorption between the pristine CNC and liposome as a function of pH, we used 1% Rhodamine (Rh) to label three different kinds of liposomes, which are DOPC, DOTAP, and DOPG. Then, we respectively mixed our pristine CNC with each of the liposomes. After centrifugation, the conjugation of CNC and liposome was spun down and the free liposomes remained in the supernatant. If the liposome was adsorbed by CNC completely, the supernatant would be dark under UV light suggesting the low fluorescence intensity. The fluorescence intensity of the supernatant was then measured to quantify adsorption of liposome by pristine CNC.

Figure 11C shows that for DOTAP, it can be adsorbed completely in the whole pH range tested. This is because the supernatant fluorescence is completely dark. The supernatant fluorescence was then quantified in figure 11C, and this result also supports full adsorption. In addition, the average size of liposome increased from around 100 nm for free liposome to over 1000 nm when mixed with CNC (Figure 11B), indicating the aggregation between pristine CNC and DOTAP. To further understand the interaction in this system, zeta-potential was characterized as well. The zeta-potential of the pristine CNC at pH 7 is -34.9 mV in 10mM HEPES buffer at room temperature (Table 2) due to the presence of functional groups, such as sulfur groups ($-SO_4^{2-}$) on the surface of CNC. As for pure DOTAP, the zeta-potential is around 22.5 mV at pH 7 (Table 3) due to the positive charged head groups. We reason that the interaction between pristine CNC/DOTAP complexes can probably be electrostatic interaction due to the positive charges on the surface of DOTAP and the negative charges on the surface of CNC.

As a comparison, there is almost no adsorption for DOPG (zeta potential = - 90.6 mV at pH 7) (Table 3) from Figure 11A, which means there is no interaction between pristine CNC and DOPG. It is mainly due to the same negative charges on the surface of pristine CNC.

Next we studied zwitteionic liposome, DOPC. When mixed with pristine CNC and centrifugation, the supernatant of the samples was dark (Figure 11C) at pH 3 while it

was bright at pH 7 under the same UV light excitation, suggesting that the

supernatant at pH 7 contained more free liposome than the supernatant at pH 3.

Figure 11A also shows the similar result that there was some adsorption at lower pH.

The adsorption efficiency goes down gradually from 90% to 10% while the pH

increases from 3 to 8 for DOPC. In addition, the particle size decreased from over

1000 nm at pH 3 to around 200 nm at pH 8 (Figure 11B), indicating conglomeration

disappeared as pH increased.

One possible explaination for this phenomenon could be attributed to the

unique structure of DOPC. DOPC is a zwitterionic liposome (zeta potential= -2.3 mV

at pH 7) with negatively charged phosphate and positively charged quaternary

ammonium. Phosphate is a weak acid and can be partially protonated at low pH, for

example, at pH 3. In this case, DOPC displays partial positive charges. So it is more

likely to be adsorbed by the anionic pristine CNC. However, the degree of

protonation will be reduced when pH increases, which will weaken the capability to

form the complex with pristine CNC. In addition, researchers have found that the

binding between DOPC and nanoparticles would be stronger when the surface of

nanoparticles is anionic due to the cationic end group of DOPC[46]. A scheme

summarizing the interaction is shown in Scheme 6.
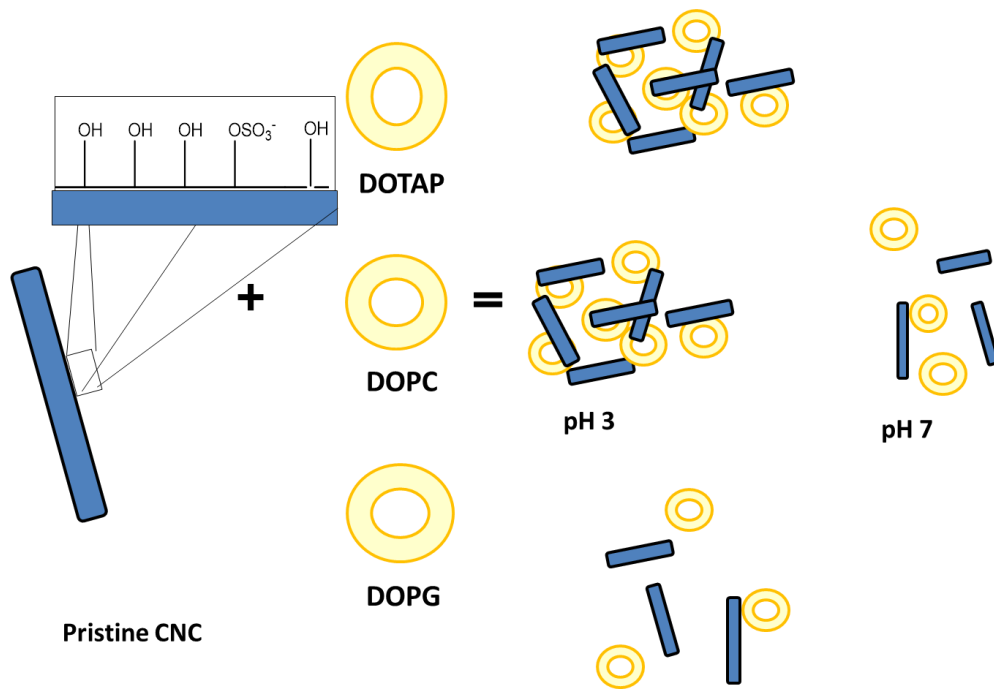
Scheme 6. Schematics of adsorption of three types of liposomes onto pristine CNC.
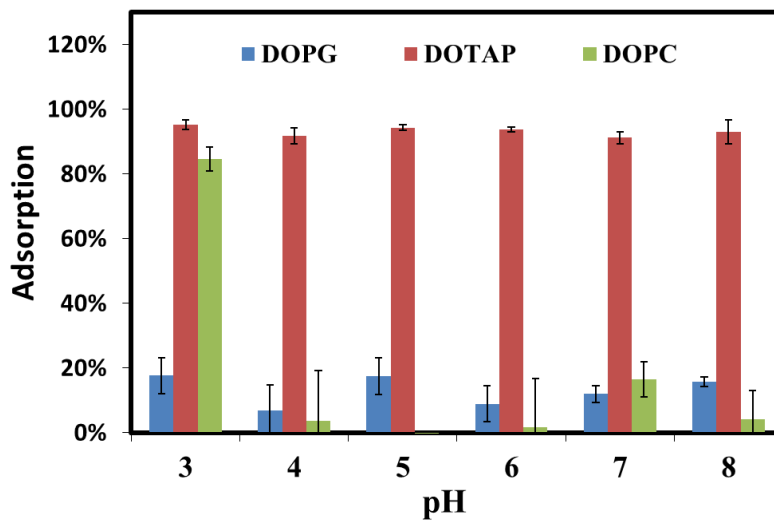
TEMPO-oxidized CNC

Figure 12. Adsorption of three types of liposomes by TEMPO CNC as a function of pH.

We next studied with TEMPO-oxidized CNC containing carboxyl groups on the surface to see the adsorption of three liposomes as a function of pH using fluorescence techniques. TEMPO CNC (zeta-potential=-36.4 mV at pH 7) (Table 2), of which has a zeta-potential close to pristine CNC, was prepared by oxidation of the hydroxyl groups on the surface of pristine CNC to carboxyl groups. Since the surface charge remains the same, the adsorption behavior between DOTAP and TEMPO-CNC is similar to the pristine CNC. Our data showed that DOTAP could be adsorbed by TEMPO CNC no matter the pH used (Figure 12), while DOPG could not. This can also be explained by electrostatic interactions.

However, there was a little difference for DOPC part. We can see (Figure 12) that the adsorption of DOPC is over 90% at pH 3 for TEMPO CNC. When we increased the pH to 4, the adsorption disappeared (Figure 12), which showed an abrupt change due to the change of pH. However, the adsorption degree of pristine CNC to DOPC decreased gradually when the pH increased, suggesting that TEMPO CNC/DOPC complexes were more sensitive to pH.
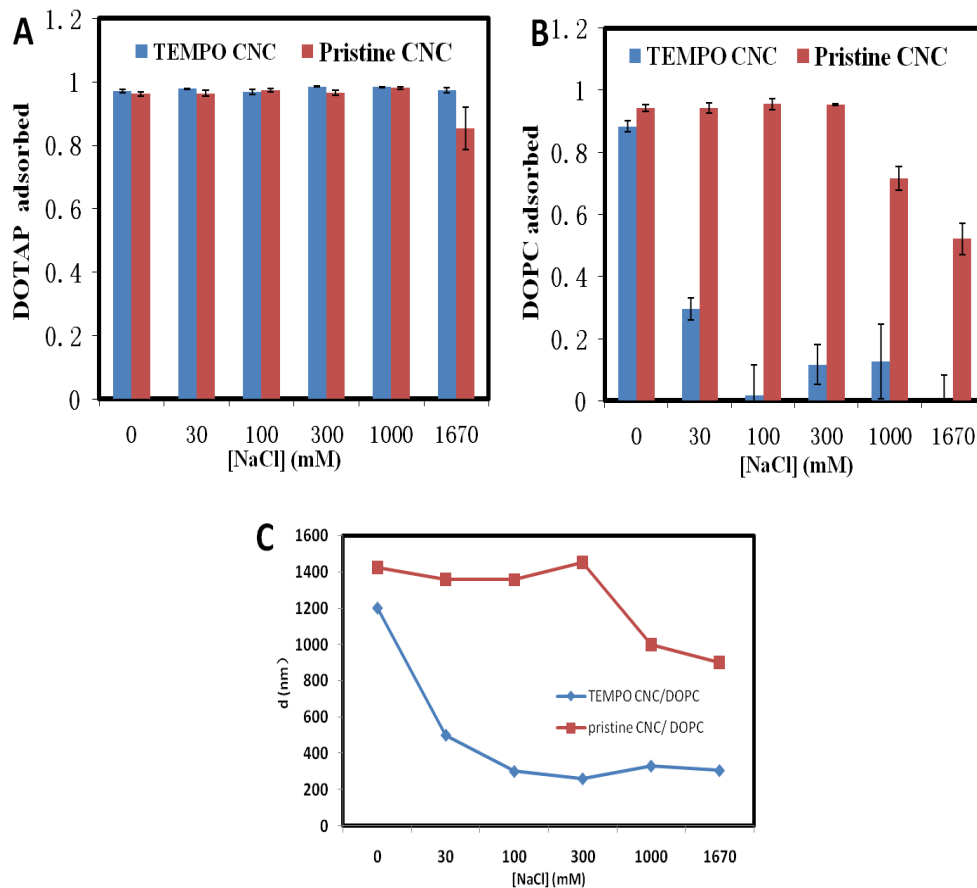
Figure 13. A) Adsorbed DOTAP by TEMPO CNC and pristine CNC as a function of salt

concentration at pH 7. B) Adsorbed DOPC by TEMPO CNC and pristine CNC as a function of salt

concentration at pH 3. C) Change of the complex size between DOPC and pristine CNC or TEMPO

CNC as a function of salt at pH 3.

After the adsorption behavior between CNC and liposomes was confirmed, we

tried to understand the driving force for the formation and control of the complex.

Electrostatic interaction or hydrogen binding are the most likely drive behind the

phenomenon. Here, the electrostatic interaction was first investigated. Research

shows that salt can reduce the electrostatic contributions to stability under

conditions with few total charges, but cannot eliminate electrostatic effects in highly

charged systems[48].

Different concentrations of salt from 0 mM to 1670 mM were added to CNC to

detect if it could affect the interaction. The study was carried out at neutral pH (pH 7)

for DOTAP since it can be adsorbed by pristine CNC and TEMPO-CNC at all pH ranges

(from pH 3-8). For DOTAP system, the adsorption remains 100% in TEMPO CNC even

when increasing the salt concentration to 1670 mM (Figure 13A), which means that

adsorption still exists even the salt concentration is very high, suggesting a strong

electrostatic interaction between TEMPO CNC and DOTAP. However, for pristine CNC,

the adsorption decreased to around 76% due to high salt concentration (Figure 13A).

For the DOPC/CNC system, the experiment was carried out at pH 3 because

DOPC can only be adsorbed in the acidic condition. Figure 13B shows that salt could

disrupt the adsorption between TEMPO CNC and DOPC in a very low concentration

(30 mM). In addition, the particle size of TEMPO CNC/DOPC complex shows a large

decrease from 1200 nm to around 500 nm when the salt concentration is 30mM

(Figure 13C). However, further increasing the salt concentration does not influence

the adsorption of DOPC/pristine CNC complex until the salt concentration reaches

1000 mM (Figure 13B). The particle size of the DOPC/pristine CNC complex is also

consistently over 1000 nm when the salt concentration is lower than 1000 mM. A

conclusion can be made that the concentration of salt has more influence on TEMPO

CNC/ DOPC system than the pristine CNC/ DOPC system at pH 3.

Different structures of CNC are highly responsible for this phenomenon. TEMPO CNC contains carboxyl groups after surface modification while pristine CNC does not. The zeta potential of TEMPO CNC at pH 3 is around -12.4 mV (Figure 11B) due to the protonation of -COOH on the surface of TEMPO CNC compared with the zeta potential of pristine CNC, which is around -27.4mV due to the negative sulfate groups on its surface. In addition, the zeta potential of DOPC is around 2.73 mV at pH 3. Therefore, the interaction between DOPC and TEMPO CNC is weaker and more prone to be further weakened by salt than that between DOPC and pristine CNC. In this case, we deduced that the driving forces between pristine CNC/DOPC and TEMPO CNC/DOPC complexes were mainly electrostatic interactions due to the opposite surface charges.

GTMAC-modified CNC
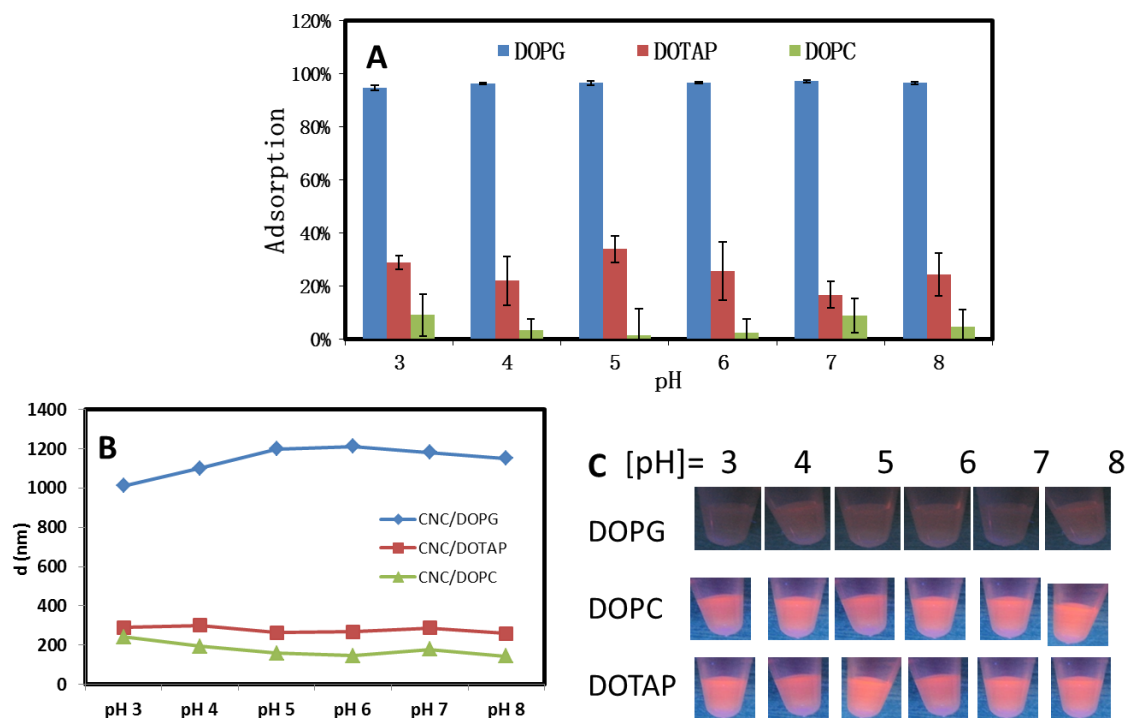
Figure 14. A) Adsorption of three types of liposomes by GTMAC-modified CNC as a function of pH.

B) Change of the complex size between GTMAC CNC and three types of liposomes as a function

of pH. C) Photographs of Rh-labeled liposomes interacting with GTMAC CNC as a function of pH.

High fluorescence indicates week interaction.

To investigate the absorption behavior between liposomes and positively

charged CNC, GTMAC-modified CNC was used to explore the interaction. The

zeta-potential of GTMAC CNC (around 22.9 mV at pH 7) showed that there are some

positive charges on the surface of CNC, which was different from pristine CNC and

TEMPO CNC. The supernatant is quite dark (Figure 14C) under all pH ranges

indicating the adsorption between GTMAC CNC and DOPG. We can see from Figure

14A that the DOPG was adsorbed almost 100% from pH 3 to pH 8. At the same time, aggregation was also confirmed by the size of complex which is over 1000 nm (Figure 14B). Electrostatic interaction is one of the possible driving forces because the GTMAC CNC is positively charged while the DOPG (zeta-potential=-80mV) is negatively charged.

However, about 20% of DOTAP, of which the zeta-potential is always positive ranging from pH 3 to pH 8, can still be adsorbed by GTMAC CNC as shown in Figure 14A. This might be due to the remained sulfate groups on the surface of GTMAC CNC. The positively charged DOTAP can still have some interaction with the sulfate groups in GTMAC CNC, which leads to a partial adsorption. The supernatant fluorescence of DOPC system was quite strong (Figure 14C) and the size of the complex remained unchanged (Figure 14B), suggesting no interaction with GTMAC CNC.
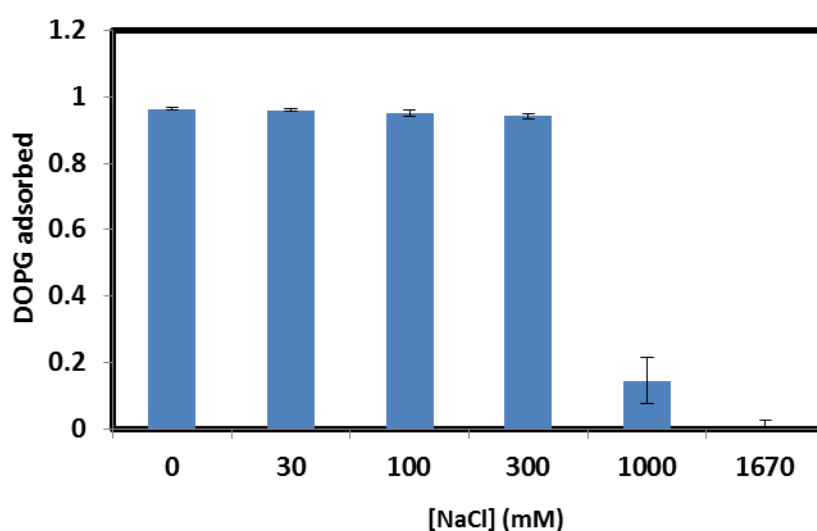
Figure 15. A) Adsorbed DOPG liposomes by GTMAC CNC as a function of salt concentration at pH 7.

Then, the salt-dependent experiment on DOPG with GTMAC CNC at pH 7 was carried out. The results are listed in Figure 15. It shows that the interaction between these two particles could be destroyed when the concentration of salt is over 1000 mM. Therefore, electrostatic interaction between this system is confirmed.

Leakage test and urea test

Figure 16. A) Calcein loaded DOPC and DOPG liposome leakage test. At time 5 minute, liposomes were mixed with CNC, and at 30 min, Triton X-100 was added. B) Free Calcein with pristine CNC and

GTMAC CNC. C) Calcein loaded DOPG liposome test. At time zero, DOPG liposomes were mixed with

CNC, same amount of DOPG was added into system every 5 minutes until at 30 min, Triton X-100 was

added. D) DOPC dispersed in 8M urea, E) with pristine CNC, F) with TEMPO CNC.
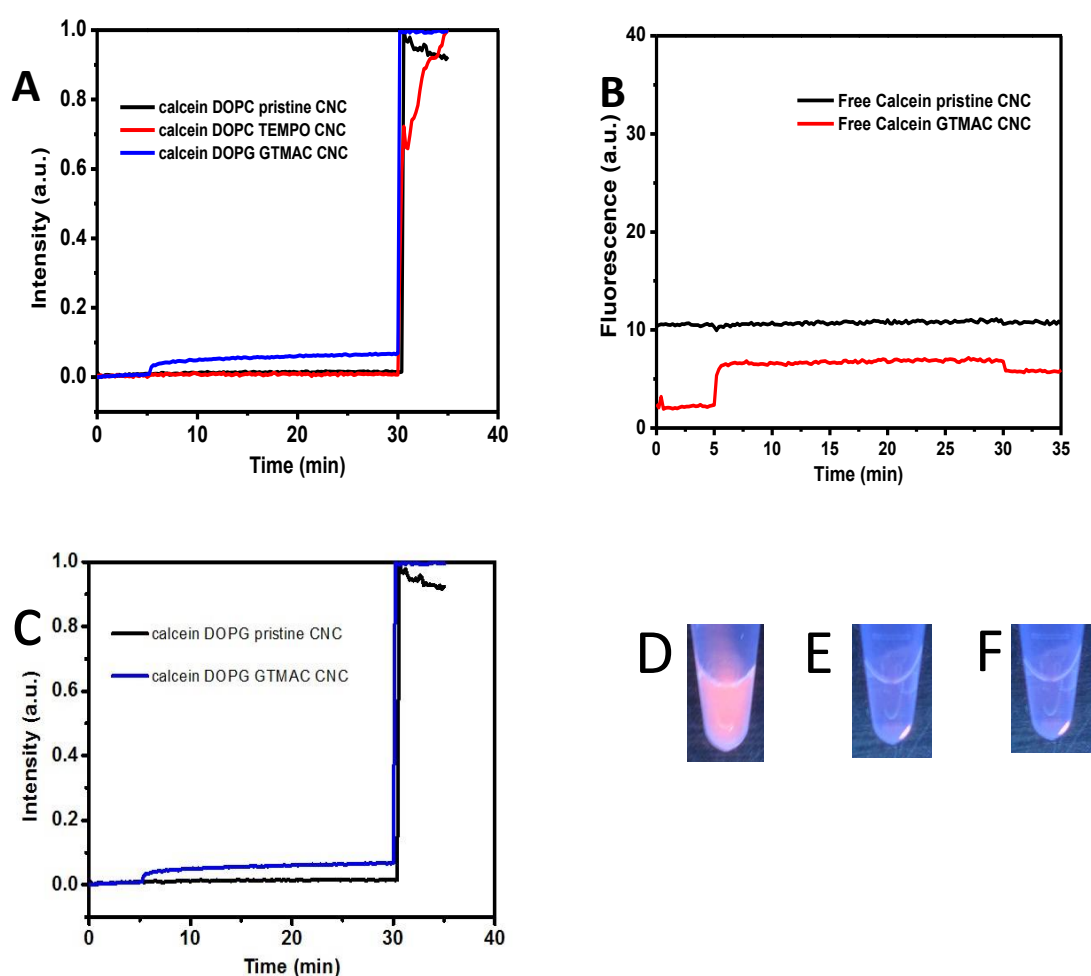
After understanding the adsorption of CNC onto a liposome surface, the next

question is whether such adsorption can induce liposome leakage or pore formation.

In order to test whether CNC would induce pore formation or break the membrane

of liposomes, the following experiment was performed. We encapsulated 100 mM

calcein inside liposomes to obtain the self-quenching effect. Fluorescence

enhancement is achieved only after the dye leaking out from the liposome. The

leakage of different kinds of liposomes was monitored by fluorescence enhancement.

Figure 16A shows that, for DOPC, there was almost no leakage when adding pristine

CNC or TEMPO CNC into the sample at 5 min. In contrast, for DOPG, the fluorescence

intensity improved a little bit by adding GTMAC CNC. In order to confirm the

interaction between GTMAC CNC/DOPG complexes, more GTMAC CNC was

continuously introduced into the system. However, the leakage did not increase

correspondingly (Figure 16C), indicating that it might not be that GTMAC CNC causes

the leakage of calcein from the liposomes.

To further identify the interaction between free calcein and CNC, a

fluorescence test using free calcein with GTMAC CNC and pristine CNC was carried

out. A small increase was shown in Figure 16B between free calcein and GTMAC CNC.

Compared with consistent figure for GTMAC CNC in Figure 16A, a conclusion can be made that the increasing fluorescence intensity from GTMAC CNC/DOPG is due to adsorption between free anionic calcein outside the liposome and cationic GTMAC CNC. However, compared with the intensity of fluorescence of full rupture at 30 min by adding Triton X-100, the change of fluorescence induced by GTMAC CNC was very small.

According to result from pH-dependent experiments, it indicated that DOPC can have stronger interaction with pristine CNC and TEMPO CNC at low pH (pH 3). In order to understand the main attractive force between CNC and liposomes, urea was added to further test hydrogen bonding. DOPC was incubated with pristine CNC at pH 3 in the presence of 8M urea. Figure 16E shows that the supernatant was clear while there was a very bright light on the bottom under UV light, which came from the complexes between pristine CNC and DOPC. Compared with the tube in Figure 16 D without CNC which was all bright, conclusion can be made that urea did not destroy the interaction between pristine CNC and DOPC. A similar phenomenon was also observed for the TEMPO CNC (Figure 16 F). Urea is known to be one of the strongest hydrogen-bonding-forming substances, which can break the hydrogen bonding in other systems[49]. As a result, hydrogen bonding does not play an important role between DOPC and negatively charged CNC.

Conclusions

In this work, the interaction between three types of CNC and three types of liposomes were systematically studied.

For pristine CNC and TEMPO CNC, they have electrostatic interaction with cationic liposome (DOTAP) due to the opposite surface charges. Similarly, the cationic CNC (GTMAC CNC) can also interact with anionic liposome (DOPG). The type of the interaction could possibly be the electrostatic adsorption instead of hydrogen bonding since it can be affected by salt but not urea. In addition, the size of the complex are over 1000 nm indicating that these complexes are not colloid stable and easy to aggregate, which is not favorable for a drug delivery system.

For DOPC (zwitterionic), it can only interact with pristine CNC in low pH. Meanwhile, the adsorption decreases gradually when the pH increases due to the protonation effect on DOPC. DOPC has no interaction with pristine CNC at normal pH (pH 7). The results of leakage test also tell that CNC has no damage to the membrane of liposomes upon adsorption.

In this system, we found that CNC and liposomes can truly have some interactions. It is very useful to take cryo-TEM images on the complex to confirm formation between CNC and liposomes. Besides, liposomes are good drug carriers. However, they cannot delivery proteins and the drug loading efficiency is low. With the help of CNC, this system could carry more drugs and increase the efficiency. One

48

of the big problems is that the size of the complex is not colloid stable and can be up to 1000 nm, which is too big to go into the cells. Controlling the size of CNC/liposome system is the key to solve this problem in drug delivery. One of the suggestions is to decreasing the concentration of CNC to form a stable particle. For DOPC, it can only interact with pristine CNC in low pH. Compared with the pH 7 for human bodies, conclusion can be made that DOPC is not an ideal carrier in this system to loading drugs.

References

(1) Sullivan, A. C. O. *Cellulose* **1997**, 173–207.

(2) Azizi Samir, M. A. S.; Alloin, F.; Dufresne, A. *Biomacromolecules* **2005**, *6*, 612–626.

(3) Nishiyama, Y. *J. Wood Sci.* **2009**, *55*, 241–249.

(4) Habibi, Y.; Lucia, L. A.; Rojas, O.J. *Chem.Rev.* **2010,** *110*, 3479–3500.

(5) Klemm, D.; Kramer, F.; Moritz, S. ; Lindström, T. ;Ankerfors, M. ; Gray, D. *Angew. Chem. Int. Ed.* **2011,** *50*, 5438–5466.

(6) Azizi Samir, M.A.S.; Alloin, F.; Dufresne, A. *Biomacromolecules* **2005,** *6*, 612–626.

(7) Peng, B. L.; Dhar, N.; Liu, H. L.; Tam, K. C. *Can. J. Chem. Eng.* **2011**, *89*, 1191–1206.

(8) Lam, E.; Male,K. B.; Chong, J. H.; Leung,A. C.; Luong,J. H., *Trends in biotechnology* **2012,** *30*, 283-90.

(9) Elazzouzi-Hafraoui, S.; Putaux, J.; Heux, L. *J. Phys. Chem. B.* **2009,** *113,* 11069–1107

(10) Moon, R.J.; Martini, A.; Nairn, J.; Simonsen, J.; Youngblood, J. *Chem. Soc. Rev.* **2011,** *40*, 3941–3994.

(11)Filson, P. B.; Dawson-Andoh, B. E. *Bioresour. Technol.* **2009**, *100*, 2259–2264.

(12) Wang, N.; Ding, E.; Cheng, R. *Langmuir* **2008**, *24*, 5–8.

(13) Beck-Candanedo, S.; Roman, M.;Gray, D.G.*Biomacromolecules* **2005**,6, 1048–1054.

(14) Dong, X.M.; Revol, J.-F.; Gray, D.G. *Cellulose* **1998,** *5*, 19–32.

(15) Elazzouzi-Hafraoui, S.;Nishiyama, Y.;Putaux, J.-L.;Heux, L.; Dubreuil, F.; Rochas, C. *Biomacromolecules* **2008,** *9*, 57–65.

(16) Roman, M.; Winter, W. T. *Biomacromolecules* **2004**, *5*, 1671–1677.

(17) Filpponon, I. The Synthetic Strategies for Unique Properties in Cellulose Nanocrystal Materials, North Carolina State University, **2009.**

(18) Lu, P.; Hsieh, Y.-L. *Carbohydr. Polym.* **2010**, *82*, 329–336.

(19)Araki, J.; Wada, M.; Kuga, S.; Okano, T. *Colloids Surfaces A Physicochem. Eng. Asp.* **1998**, *142*, 75–82.

(20) Habibi, Y.; Chanzy, H. Vignon, M.R. *Cellulose* **2006,** 13, 679–687.

(21) Hasani, M.; Cranston, E.D.; Westman, G.; Gray, D.G. *Soft Matter* **2008**,4, 2238–2244.

(22) Goussé, C.; Chanzy, H.; Excoffier, G.; Soubeyrand, L.; Fleury, E. *Polymer* **2002,**43,2645–2651.

(23) Junior de Menezes, A.; Siqueira, G.; Curvelo, A.A.S.; Dufresne, A. *Polymer* **2009,**50,4552–4563.

(24) Pandey, J. K.; Chu, W.S.; Kim, C.S.; Lee, C.S.; Ahn, S.H. *Composites Part B.* **2009,** 40, 676–680.

(25) Siqueira, G.; Bras, J.; Dufresne, A. *Biomacromolecules* **2009,**10, 425–432.

(26) Lam, E.; Male, K.B.; Chong, J.H.; Leung, A.C.W.; Luong, J.H.T. *Trends in Biotechnology* **2012,**30,283–290.

(27) Katoa, Y.; Matsuoa, R.; Isogaib, A. *Carbohydrate Polymers* **2003,**51,69–75

(28) Zaman, M.; Xiao, H.; Chibante, F.; Ni, Y. *Carbohydr. Polym.* **2012**, *89*, 163–170.

(29) Habibi, Y.; Heim, T.; Douillard, R. *J. Polym. Sci. Part B* **2008**, 1430–1436.

(30) Araki, J.; Wada, M.; Kuga, S. *Langmuir* **2001**, *17*, 21–27.

(31) Mangalam, A. P.; Simonsen, J.; Benight, A. S. *Biomacromolecules* **2009**, *10*, 497–504.

(32) Lin, N.; Chen, G.; Huang, J.; Dufresne, A.; Chang, P. R. *J. Appl. Polym. Sci.* **2009**, *113*, 3417–3425.

(33) Siqueira, G.; Bras, J.; Dufresne, A. *Langmuir* **2010**, 26, 402–411.

(34) Fahy, E.; Subramaniam, S.; Murphy, R.; Nishijima, M.; Raetz, C.; Shimizu, T.; Spener, F.; Van Meer, G.; Wakelam,; Dennis, E.A *J. Lipid Res.* **2009,** 50, 9-14.

(35) Subramaniam, S.; Fahy, E.; Gupta, S.; Sud, M.; Byrnes, R.W.; Cotter, D. *Chem. Rev.* **2011,** 10, 6452–6490.

(36) Salim, M.; Minamikawa, H.; Sugimura, A.; Hashim, R. *Med.Chem.Commun*. **2014**, 5, 1602-1618

(37) Bangham, A. D. *Liposomes in Biological Systems.***1980,** 1-24

(38) Gregoriadis,G.; Allison, A. *Pharmacol. Res.* **1999,** 51, 691-743.

(39) Allen, T.; Cheng, W.; Hare J.; Laginha K. *Anticancer. Agents.Med. Chem.* **2006,** 6, 513-23.

(40) Allen, T.; Hansen, C. *Biomembranes* **1991**, 068, 133-141.

(41) Drummond, D.C.; Zignani, M.; Leroux, J.C. *Lipid. Res*. **2000,**39, 409.

(42) Li, W.; Szoka, F.C. *Pharm. Res.* **2007,**24, 438-449

(43) Frost, R.; Jonsson,G. E.; Chakarov, D.; Svedhem, S. Kasemo, B. *Nano. Lett.* **2012,** 12, 3356–3362.

(44) Zhou, X.; Moran-Mirabal, J. M.; Craighead, H. G.; McEuen, P. L.*Nat.Nanotechnol.,* **2007,** 2, 185–190.

(45) Wang, F.; Liu, J.W. *Nanoscale*, **2013,** 5, 12375

(46) Yu, Y.; Anthony, S.M.; Zhang, L.F.; Bae, S.C.; Granick, S. *J. Phys. Chem. C,* **2007,** 111, 8233-8236

(47) Liang,X.; Li, X.; Yue,X.; Dai, Z. *Angew. Chem., Int. Ed.* **2011** ,50 ,11622 .

(48) Stellwagen, E.; Stellwagen, N.C. *Biophys J.* **2003**, 84, 1855-1866.

(49) Mirsky, A.E.; Pauling, L. *Proc. Nail. Acad. Sci.* **1936**, 22, 439-447